Low molecular-weight chitosan as a pH-sensitive stealth coating for tumor-specific drug delivery

Zohreh Amoozgar[1], **Joonyoung Park**[1], **Qingnuo Lin**[1], and **Yoon Yeo**[1,2,*]

[1]Department of Industrial and Physical Pharmacy, Purdue University, 575 Stadium Mall Drive, West Lafayette, IN 47907, USA

[2]Weldon School of Biomedical Engineering, Purdue University, West Lafayette, IN 47907, USA

Abstract

When a nanoparticle is developed for systemic application, its surface is typically protected by polyethylene glycol (PEG) to help their prolonged circulation and evasion of immune clearance. On the other hand, PEG can interfere with interactions between nanocarriers and target cells and negatively influence the therapeutic outcomes. To overcome this challenge, we propose low molecular-weight chitosan (LMWC) as an alternative surface coating, which can protect the nanomedicine in neutral pH but allow cellular interactions in weakly acidic pH of tumors. LMWCs with a molecular weight of 2–4 kDa, 4–6.5 kDa, and 11–22 kDa were produced by hydrogen peroxide digestion and covalently conjugated with poly(lactic-co-glycolic acid) (PLGA). Nanoparticles created with PLGA-LMWC conjugates showed pH-sensitive cell interactions, which enabled specific drug delivery to cells in a weakly acidic environment. The hydrophilic LMWC layer reduced opsonization and phagocytic uptake. These properties qualify LMWCs as a promising biomaterial for pH-sensitive stealth coating.

Keywords

pH-sensitive; stealth; nanoparticles; low molecular-weight chitosans; tumor-specific drug delivery

INTRODUCTION

Toxic side effects are one of the main challenges during systemic chemotherapy. To increase tumor uptake of anti-neoplastic agents and decrease side effects on healthy tissues, nanoparticulate drug carriers (nanocarriers) have been widely explored. In particular, polymeric nanoparticles (NPs), micelles, or liposomes are frequently used for tumor-specific drug delivery, due to their small size amenable to systemic application and the ability to accommodate a wide range of ligands that can improve interactions with target tissues.

Irrespective of particle type and surface ligands, the majority of systemically-administered nanocarriers depend on the leakiness of the vasculature surrounding tumors to reach the targeted tumors.[1–3] Therefore, prolonged circulation and reduced immune clearance are primary design criteria for tumor-targeted NPs. Since hydrophobic surfaces of NPs cause non-specific interactions with healthy tissues[4] and premature clearance by the reticuloendothelial systems (RES),[5] NPs are almost always coated with polyethylene glycol

(PEG),[6] which forms a hydrated shell. The non-fouling or 'stealth' PEG coating provides NPs with a steric barrier that protects them from opsonization and cellular interactions.[7]

However, PEG is not free of limitations. PEG can interfere with a NP's interaction with target cells,[8–10] thus compromising efficacious drug delivery to the cells. This property, the so called "PEG dilemma",[11] negatively influences the therapeutic outcomes, especially when cellular uptake of the carrier is critical to the biological effects of the payloads (e.g., gene therapeutics, efflux pump substrates) and/or when the NPs are constantly subject to removal from target tissues. Several attempts have been made to enable conditional unmasking of the PEGylated NPs and enhance the cellular interaction of the NPs at target tissues. Such efforts include modification of the NP surface with 'sheddable' PEG, where the linkers between the surface and PEG are cleaved in response to unique conditions of target tissues, such as pH.[12, 13] The reported range of tumoral extracellular pH values is 5.8–7.6, with a median value of 7.0^{14} or $6.8–7.2^{13}$, as compared to 7.4–7.5 of normal tissues. Therefore, PEG is conjugated to liposomes via a hydrazone linker, which cleaves at pH 5–6,[15–17] or electrostatically attached to micelles via a pH-sensitive block, which detaches from the micelles as the pH drops to below pH 6.6.[18]

In this study, we hypothesized that low molecular weight chitosan (LMWC) could be used as an alternative stealth coating, responsive to the pH of target tumors. Chitosan is a linear copolymer of glucosamine and N-acetylglucosamine, obtained by partial (>50%) N-deacetylation of chitin, the second most abundant natural polymer. The primary amines provide chitosan with a unique pK_a of 6.5, which matches the weakly acidic pH of tumor tissues.[13] In the acidity of the extracellular matrix of solid tumors, chitosan is protonated and can adhere to cells via electrostatic interactions with glycocalyx on the cell membrane. Moreover, the presence of primary amine groups facilitates covalent conjugation of chitosan to polymers. The ideal pH-sensitivity, chemical reactivity, and cost-effectiveness make chitosan an attractive biomaterial for NP surface modification.

Here, LMWCs with various molecular weights (MWs) were covalently conjugated to poly(lactic-co-glycolic acid) (PLGA). The NPs prepared with the PLGA-LMWC conjugates were tested with respect to the physical and chemical properties, pH-sensitivity in cell-NP interaction and drug delivery, and the potential to provide a stealth surface on NPs, in comparison with PLGA NPs with bare surface and/or PLGA NPs covered with PEG.

EXPERIMENTAL SECTION

Materials

Paclitaxel (PTX) was a gift of Samyang Genex Corp. (Seoul, Korea). 1-hydroxybenzotriazole hydrate (HOBT) was purchased from Spectrum Chemical Mfg. Corp. (Gardena, CA, USA), and poly(lactic-co-glycolic acid) (PLGA, lactic acid:glycolic acid = 50:50, with a carboxylic acid terminus, 4.2 kDa) was from Durect Corporation (Birmingham, AL, USA). Chitosan (15 kDa; deacetylation degree: 87%) was purchased from Polysciences, Inc (Warrington, PA, USA). Chitosan (50–190 kDa; deacetylation degree: 83%), 1-ethyl-3-[3-dimethylaminopropyl]carbodiimide (EDC), sodium dodecyl sulfate (SDS), dichloromethane (DCM), methanol, acetonitrile (AcN), and N,N,N',N'-tetramethylethylenediamine (TEMED) and standard PEGs with known MWs were purchased from Sigma-Aldrich (St. Louis, MO, USA). Dimethyl sulfoxide (DMSO) was purchased from Mallinckrodt Baker Inc. (Phillipsburg, NJ, USA). (3-(4,5-Dimethylthiazol-2-yl)-2,5-diphenyltetrazolium bromide) (MTT) was purchased from Invitrogen (Eugene, OR, USA). 1,5-bis-4, 8-dihydroxyanthracene-9,10-dione (DRAQ-5) was purchased from Axxora LLC (San Diego, CA, USA). Amine-functionalized

polyehthylene glycol (methoxy-PEG-amine, HCl salt, 5kDa) was purchased from JenKem technology USA (Allen, TX, USA).

Production and characterization of low molecular-weight chitosans (LMWCs)

Chitosan (50–190 kDa) was digested with hydrogen peroxide (H_2O_2, 33%) to produce LMWCs. H_2O_2 30 mL was added to 10 g of chitosan dissolved in 400 mL of acidified water (pH 3) and stirred vigorously. The reactions were quenched by adding 50 mL of methanol after 1, 3.5, or 9 hours, and the pH was adjusted to 7. The LMWC digested for 1 hour was purified by alternating alkaline precipitation (pH 9) and redissolution in acidic solution (pH 3), which was repeated at least 5 times. The final pH was adjusted to 5 with dilute HCl, and the resulting solution was lyophilized. The LMWCs digested for 3.5 or 9 hours were dialyzed against water using a dialysis bag with a molecular weight cut-off (MWCO) of 3.5 kDa or 1 kDa, respectively.

MWs of the LMWCs were determined by gel permeation chromatography (GPC) equipped with two 7.8 mm × 30 cm TSKGel G3000pwxl columns and a guard column (Tosoh Biosciences, King of Prussia, PA, USA) on an Agilent 1200 HPLC system operated with Agilent ChemStation and GPC data analysis software (Santa Clara, CA, USA). The eluent was phosphate buffered saline (PBS, 10 mM phosphate, pH 7.4) and flowed at 1 mL/min. PEGs with known MWs (0.4, 1, 1.9, 4.02, 6.45, 11, and 22 kDa) were prepared as 1 mg/mL solution in PBS to produce a calibration curve. The LMWCs were prepared as 1 mg/mL solution in PBS and analyzed with GPC. The LMWCs were labeled as $LMWC_{2-4k}$, $LMWC_{4-6.5k}$, and $LMWC_{11-22k}$, according to the MW ranges determined by GPC.

Water solubilities of LMWCs and the parent chitosan were monitored by observing the turbidity change of the chitosan solutions varying the pH. The chitosans were dissolved in 10 mM NaCl (pH 3). The transmittance of a solution was measured at the wavelength of 500 nm, increasing its pH from 3 to 11 with 0.1 N NaOH.

PLGA modification

PLGA-LMWC conjugates: LMWC (200 mg) was dissolved in 20 mL of water (pH 5) and added to 40 mL of DMSO under stirring. PLGA (500 mg, 0.12 mmol) was dissolved in 2 mL of DCM, to which HOBT (74.3 mg, 0.55 mmol) dissolved in 1 mL DMSO, EDC (106.2 RL, 0.6 mmol) in 1 mL water, and TEMED (269.9 RL, 1.8 mmol) in 1 mL DMSO were sequentially added to convert the carboxyl group of PLGA to HOBT-ester, a good leaving group. The activated PLGA solution was added dropwise to the LMWC solution and stirred at pH 5–5.5 overnight. The resulting product, PLGA-LMWC conjugate, was dialyzed against a 50:50 mixture of water and DMSO using a dialysis bag with a MWCO of 3.5 kDa or 7 kDa to remove the unreacted LMWC and PLGA. During the last dialysis, DMSO was exchanged with water, and the aqueous solution was lyophilized. Conjugation of LMWC and PLGA was confirmed by Fourier transform infrared spectroscopy (FTIR) using a Bio-Rad FTS 6000 spectrophotometer (Bio-Rad Laboratories, Hercules, CA).

PLGA-PEG conjugate: PLGA (100 mg, 0.024 mmol) and HOBT (5 mg, 0.04 mmol) were dissolved in 5 mL DMSO under stirring. EDC (8.5RL, 0.05 mmol) and N,N-diisopropylethylamine (12.5RL, 0.07 mmol) were sequentially added to the solution and stirred for 1 hour to form activated PLGA. Methoxy-PEG-amine (200 mg, 0.04 mmol) dissolved in 1 mL DMSO was added dropwise to the reaction mixture and stirred overnight. PLGA-PEG was dialyzed against a 75:25 mixture of water and DMSO using a dialysis bag with a MWCO of 10,000 Da to remove the unreacted PLGA and PEG. Finally, DMSO was exchanged with water, and the aqueous solution was freeze-dried. Percent conjugation of PEG to PLGA was quantified by ^{1}H-NMR spectroscopy after NP formation.

Preparation and characterization of NPs

NPs were prepared with PLGA, PLGA-LMWC conjugates, or PLGA-PEG conjugate, and named as PLGA NP, PLGA-LMWC NP, or PLGA-PEG NP, respectively. PLGA-LMWC NPs were further distinguished according to the used LMWC as PLGA-LMWC$_{2-4k}$ NP, PLGA-LMWC$_{4-6.5k}$ NP, and PLGA-LMWC$_{11-22k}$ NP. Each polymer (20 mg) was dissolved in a mixture of 0.5 mL DMSO, 0.5 mL DCM, and 0.1 mL water. The polymer solution was added to 3 mL of water containing 5% polyvinyl alcohol (PVA) and emulsified for 1 min with a Vibra-Cell probe sonicator (Sonics, Newtown, CT, USA) at 80% amplitude and on a 4-sec on and 2-sec off pulse mode. The polymer emulsion was stirred for 3 hours to evaporate DCM, and then washed with distilled water four times to remove trace DCM, DMSO, and PVA. When paclitaxel (PTX) was encapsulated, 2 mg of PTX (or 1.2 mg PTX) was dissolved in 0.5 mL DCM and combined with 20 mg PLGA (or 20 mg PLGA-LMWC$_{2-4k}$) dissolved in a mixture of 0.5 mL DMSO and 0.1 mL water. The mixture was emulsified in the same manner as above. Alternatively, chitosan with a MW of 15 kDa (LMWC$_{15k}$) was added to the continuous phase to form physical coating on PLGA NP (PLGA/LMWC$_{15k}$ NP). PLGA/DMSO solution (20 mg/mL) was added to a 3 mL of 5% PVA solution containing 20 mg/mL LMWC$_{15k}$ and sonicated for 1 min (4-sec on and 2-sec off pulse mode, 80% amplitude). The emulsion was stirred for 3 hours and washed with distilled water. The purified NPs were suspended in phosphate buffer (1 mM, pH 7.4) or MES buffer (1 mM, pH 6.2), and their sizes and zeta potentials were measured by the Malvern Zetasizer Nano ZS90 (Worcestershire, UK). Lyophilized NPs were imaged with a FEI NOVA nanoSEM field emission scanning electron microscope (FEI Company, Hillsboro, Oregon) using the high resolution Through-the-lens detector (TLD) operating at 5 kV accelerating voltage, ~4 mm working distance, spot 3, and 30 Rm aperture.

Quantification of chitosan content in NPs

Chitosan contents in NPs were determined by the ninhydrin assay according to the previously reported method.[19] Ninhydrin reagent was prepared by dissolving hydrindantin in lithium acetate buffer. The ninhydrin reagent 0.5 mL was mixed with 0.5 ml of calibration standards or sample solutions containing lyophilized NPs (0.5 mg). The mixture was then incubated in a boiling water bath for 30 minutes and quenched by the addition of 50% ethanol. The absorbance of each solution was measured by a Cary 300 Bio UV/VIS spectrophotometer (Walnut creek, CA, USA) at 570 nm and converted to the LMWC content in NPs.

Determination of PTX loading content and in-vitro release kinetics

For determination of PTX loading in NPs, lyophilized NPs were accurately weighed, dissolved in a 50:50 mixture of AcN and water, and analyzed with high pressure liquid chromatography (HPLC) equipped with Ascentis C18-column (25 cm × 4.6 mm, particle size 5 Rm). The mobile phase was a 50:50 mixture of AcN and water and flowed at 1 mL/min. PTX peaks were detected using a UV detector at 227 nm. PTX content in NPs was calculated as a weight percentage of PTX in NPs.

For release kinetics study, PTX-laden NPs (equivalent to 3 Rg PTX) were suspended in 1 mL of PBS (10 mM phosphate, pH 7.4 and 6.2) containing 0.1% Tween 80 and incubated in a rotating shaker at 37°C. At regular time points, the NP suspension was centrifuged at 10,000 rpm for 10 min, and 0.9 mL of the supernatant was collected and replaced with fresh buffer. After the final collection at 72 hours, the remaining NP was lyophilized and dissolved in a 50:50 mixture of AcN and water. The release samples and the remaining NP were analyzed with HPLC.

Confocal microscopy of NP-cell interaction

Fluorescently labeled NPs (PLGA*-LMWC NP or PLGA* NP) were prepared by replacing 25% of PLGA-LMWC or PLGA with fluoresceinamine-labeled PLGA, prepared as reported previously.[20] Sizes and zeta potentials of NPs were measured prior to cell experiments. SKOV-3 human ovarian cancer cell line (ATCC, Manassas, VA, USA) and NCI/ADR-RES multidrug resistant ovarian cancer cells (NCI, Frederick, MD, USA) were grown in RPMI-1640 medium and DMEM/F12 without phenol red medium, respectively. J774A.1 mouse macrophages (ATCC) were grown in DMEM. All media contained 10% fetal bovine serum (FBS) and 100 units/mL penicillin and 100 ug/mL streptomycin. SKOV-3 and NCI/ADR-RES cells were seeded at a density of 50,000 cells/cm^2, and J774A.1 was at 25,000 cells/cm^2 in a 35-mm dish with a glass window (MatTek). After overnight incubation, the medium was replaced with a 0.1 mg/mL of PLGA* NP or PLGA*-LMWC NP suspension in serum-free medium (pH 6.2 or 7.4) and incubated for 3 hours. Cells were then washed with 2 mL of serum-free medium twice to remove free or loosely-bound NPs and observed using an Olympus X81 confocal microscope (Olympus, Japan). DRAQ-5 nuclear stain (1 RL) was added 2–3 minutes prior to imaging. NPs and cell nuclei were excited using a 488-nm and 633-nm laser. Their emission signals were read from 500 to 600 nm and 650 to 750 nm and expressed in green and blue, respectively.

In-vitro cell viability assay

Cytotoxicity of PTX loaded in PLGA NP or PLGA-LMWC NP was evaluated using the SKOV-3 cells based on the MTT assay. SKOV-3 cells were seeded at a density of 10,000 cells per well in a 96-well and incubated overnight in 200 RL of complete medium. The culture medium was then replaced with 200 RL of fresh medium, and its pH was adjusted to 7.4 or 6.2–6.5 (called "6.2" hereafter). Two microliters of PTX/DMSO solution or NP suspensions were added to each well to provide PTX in a final concentration ranging from 0.001 to 10,000 nM. After 72 hours of incubation, the medium was replaced with 100 RL of fresh medium containing 13% MTT and incubated for 3.5 hours. Finally, 100 RL of the solubilization/stop solution comprising 20% SDS, 0.02% v/v acetic acid, and 50% v/v DMSO was added to each well, and the absorbance was read at 560 nm by the Tecan microplate reader (Mannedorf, Switzerland). Cell viability was calculated by dividing the absorbance of treated cells by that of untreated cells after subtracting the absorbance of cell-free medium from each. Here, the untreated cells were those provided with no PTX but equally handled otherwise, and the cell-free medium was the medium mixed with MTT solution and solubilization/stop solution without cells.

The MTT assay was also carried out limiting the cell exposure to NPs to 3 hours. Briefly, SKOV-3 cells were suspended in the medium with pH 6.2 or 7.4 at a density of 50,000 cells per milliliter, to which free PTX or PTX-loaded NPs were added to provide PTX in a final concentration of 100, 1,000, or 10,000 nM. After 3 hour incubation, cells were separated from the NPs by brief centrifugation (3 min, 1000 rpm), washed with fresh medium to remove free or loosely-bound NPs, and plated at a density of 10,000 cells/well. The cells were incubated in particle-free medium (pH 6.2 or 7.4) for another 69 hours to determine the cell proliferation.

Evaluation of protein adsorption to particle surface

To evaluate the extent of protein adsorption to the particle surface, the polymers were prepared as semi-microparticles (mPs) with an average size of 700 nm, which were easier to separate and wash than NPs. PLGA or PLGA-LMWC conjugate (20 mg) was dissolved in a mixture of 0.5 mL DMSO, 0.5 mL DCM, and 0.1 mL water, and emulsified in 3 mL of 5% PVA by 2-min vortexing (PLGA and PLGA-LMWC$_{2-4k}$) or 1-min sonication at 50% amplitude on a 4 sec-on and 2 sec-off mode (PLGA-LMWC$_{4-6.5k}$). For preparation of

PLGA-PEG mP, the polymer was prepared as 40 mg/mL solution in the same solvent system and vortexed in 5% PVA solution for 2–3 seconds. After evaporating DCM for 3 hours, all mPs were washed with water 4 times. The mPs (5 mg/mL) were incubated in DMEM containing 50% FBS for 1 hour at 37°C. The mPs were then transferred to centrifugal filter tubes (0.2 Rm pore size), centrifuged at 13,000 rpm for 20 min, and washed 4 times with water. The washed mPs were lyophilized and analyzed with the micro-BCA assay for quantification of the adsorbed proteins.

RESULTS

Production and characterization of LMWCs

Chitosan (90–150 kDa) were digested by timed incubation with H_2O_2, which cleaved ether bonds between glucosamine units of chitosans.[21] The MWs of LMWCs gradually decreased with the digestion time and showed broad distribution ranging 11–22 kDa, 4–6.5 kDa, and 2–4 kDa after 1, 3.5, and 9 hour digestion, respectively. The weight-average MWs of LMWCs were 15.3 kDa (polydispersity index, PDI, Mw/Mn: 2.7), 4.3 kDa (PDI 1.9), and 2.1 kDa (PDI 1.5), respectively. The yields were 85–95% irrespective of MWs and purification methods. Water solubility of the chitosans increased as their MW decreased (Fig. 1). $LMWC_{2-4k}$ and $LMWC_{4-6.5k}$ were water-soluble at pH 3–10 and showed slight decrease in transmittance at pH above 10. Although $LMWC_{11-22k}$ was relatively more soluble than the parent chitosan (90–150 kDa), it was insoluble at pH higher than 7.6. The parent chitosan showed rapid precipitation from pH 7.0.

Characterization of PLGA-LMWC and NPs

PLGA-LMWC conjugates were produced with a yield of 25%. The conjugation of LMWC to PLGA (Scheme 1) was confirmed by the appearance of FTIR signals at 1500–1690 cm^{-1}, corresponding to amide and amine bands, and a broad signal at 3000–3700 cm^{-1} for N-H stretch (Fig. 2). The particle size of PLGA-LMWC NP varied with the MW of LMWC part of the conjugates (Table 1). $PLGA-LMWC_{2-4k}$ NP and $PLGA-LMWC_{4-6.5k}$ NP were similar to PLGA NP in size, whereas $PLGA-LMWC_{11-22k}$ NP had an average particle size greater than 400 nm. Consistent with the size measurement, PLGA NP and PLGA-$LMWC_{2-4k}$ NP looked alike under SEM in both shape and size (Fig. 3). The NPs appeared smaller (90–140 nm) than the measurement based on dynamic light scattering (170–190 nm, Table 1), suggesting some degree of NP aggregation in suspension. PLGA NP showed negative surface charges irrespective of pH, but PLGA-LMWC NP displayed opposite surface charges at pH 7.4 (slightly negative) and pH 6.2 (positive). $PLGA/LMWC_{15k}$ NP (PLGA NP physically coated with $LMWC_{15k}$) was similar to PLGA NP in both size and surface charge at either pH, indicating that $LMWC_{15k}$ added to the continuous phase did not effectively coat the PLGA NP.

LMWC content in each PLGA-LMWC NP was determined by the ninhydrin assay. The mass fractions attributable to LMWC were 5.1±1.1% for $PLGA-LMWC_{2-4k}$ NP, 8.7±1.5% for $PLGA-LMWC_{4-6.5k}$ NP, and 20.7 ± 3.5% for $PLGA-LMWC_{11-22k}$ NP (n=3 each). Assuming that the LMWC mass fraction is equivalent to the LMWC content in each PLGA-LMWC conjugate, we calculate that 17 PLGA molecules are conjugated to 1 $LMWC_{11-22k}$ chain, 13 PLGA to 1 $LMWC_{4-6.5k}$, and 18 PLGA to 1 $LMWC_{2-4k}$. However, these values remain a rough estimation due to the broad MW distribution of LMWC, which is an inherent limitation of natural polymers and H_2O_2 digestion.

NP interactions with ovarian cancer cells and macrophages

SKOV-3 and NCI/ADR-RES ovarian cancer cells were incubated with PLGA* NP and PLGA*-LMWC NPs for 3 hours at pH 6.2 or 7.4, then washed, and imaged with confocal

microscopy (Fig. 4). PLGA* NP did not much remain with cancer cells at either pH. Similarly, PLGA*-LMWC NPs incubated with cells at pH 7.4 were not seen with the cells after washing. In contrast, strong NP signals were observed in SKOV-3 cells incubated with PLGA*-LMWC NPs at pH 6.2 (Fig. 4a). NCI/ADR-RES cells showed a similar trend (Fig. 4b). In contrast, PLGA* NP was taken up by J774A.1 macrophages and appeared in the cytoplasm after 3 hour incubation at pH 7.4. Macrophage uptake of PLGA*-LMWC$_{2–4k}$ NP was not significant (Fig. 5).

In-vitro cell killing by PTX-loaded NPs

Cytotoxic effects of PTX or PTX/NPs on SKOV-3 cells were evaluated at pH 6.2 and pH 7.4. Cell proliferation was slightly attenuated at pH 6.2, but this difference was taken into account by normalizing the absorbance of treated cells to that of untreated cells, which were handled equally otherwise. The medium pH did not affect the IC$_{50}$ of PTX in SKOV-3 cells (~10 nM). Blank NPs were only slightly toxic to cells in the highest concentration used in this study.

When SKOV-3 cells were incubated with the PTX/NPs for 72 hours, the dose responses were similar to that with PTX, and neither NP showed significant dependence on pH (Fig. 6a). On the other hand, when the cell exposure to PTX/NPs was limited to 3 hours, cells incubated with PTX/PLGA NP showed only small decrease in viability even at a very high concentration (10,000 nM) (Fig. 6b). Cells incubated with PTX/PLGA-LMWC NP at pH 7.4 also showed only a moderate response to the increasing dose. In contrast, PTX/PLGA-LMWC NP at pH 6.2 showed a dose-dependent effect on cell viability, comparable to free PTX in the same pH (except for 100 nM). The results were not affected by the pH of fresh medium (6.2 or 7.4), in which cells were incubated during the subsequent 69 hours (Supporting Fig.). Depending on the nature of cellular association of PTX/PLGA-LMWC NP (endocytosis or attachment), this result can be interpreted in two ways: The NPs were endocytosed in 3 hours and not affected by the environmental pH during subsequent incubation. Alternatively, PTX/PLGA-LMWC NP captured on the cell surface in 3 hours exerted similar effects irrespective of their locations (attached to cells (pH 6.2) or separated from the cells (pH 7.4)) during the 69 hours.

PTX encapsulation and in-vitro release kinetics

PTX contents in PTX/PLGA NP and PTX/PLGA-LMWC$_{2–4k}$ NP were 6.3 ± 1.2% (n=10) and 12.6 ± 1.5% (n=6), respectively, corresponding to 69.7 ± 13.2% and 215.0 ± 34.8% of the theoretical PTX loading (9% for PTX/PLGA NP and 6% for PTX/PLGA-LMWC$_{2–4k}$ NP). The high PTX content of PTX/PLGA-LMWC$_{2–4k}$ NP indicates selective loss of PLGA-LMWC$_{2–4k}$ during multiple washing steps, attributable to hydrophilicity of the polymer. 11–12% and 76–83% of the loaded PTX were released by 3 hours and 24 hours, respectively, in PBS (pH 7.4) containing 0.1% Tween 80 (Fig. 7). The extent of drug release appeared to be relatively low in pH 6.2, but no statistical difference from that in pH 7.4 was observed. In both PTX/PLGA NP and PTX/PLGA-LMWC$_{2–4k}$ NP, no further release followed in the next 48 hours irrespective of the pH of the release medium.

Protein adsorption to particle surface

Proteins adsorbed to 1 mg of PLGA mP, PLGA-LMWC$_{2–4k}$ mP, PLGA-LMWC$_{4–6.5k}$ mP, PLGA-LMWC$_{11–22k}$ mP, and PLGA-PEG mP were 68.7 ± 7.3, 42.6 ± 3.8, 18.8 ± 2.2, 34.8 ± 5.1 and 3.9 ± 2.1 Rg per 1 mg of mPs, respectively (Fig. 8).

DISCUSSION

Chitosan is widely used for a variety of biomedical applications including drug/gene delivery and tissue engineering. In drug delivery applications, chitosan is typically used as a mucoadhesive polymer, which, when present on the surface of NPs, induces adhesive interactions between NP and mucosal epithelia.[22] Such interactions are attributed to various mechanisms, either pH-dependent or pH-independent, such as electrostatic interactions between mucins and positively charged chitosan, abundant hydroxyl and amine groups in chitosan that enable hydrogen bonding with sugar moieties in mucins,[23, 24] and flexibility of the polymer chain that allows for entanglement. The ability to establish electrostatic interactions with glycocalyx of cell membrane in acidic pH is a favorable feature for a pH-sensitive stealth coating material. However, its pH-independent interactions with cell surface glycoproteins are likely to interfere with the stealth function. Moreover, commercially available chitosans are water-insoluble in neutral pH, additionally hampering the utility of chitosan as a stealth coating. We hypothesized that reducing MW would improve water solubility of chitosan and reduce pH-independent interactions between chitosan and cells, making LMWCs suitable for pH-sensitive stealth coating.

While water-soluble in neutral pH, LMWCs did not form surface coating on PLGA NP by simple addition in the continuous phase, as typically done with relatively high MW chitosans.[25, 26] Unlike higher MW chitosans, LMWCs were easily washed away from the NP surface during the purification process, as evident from the lack of surface protonation at pH 6.2. Therefore, LMWC-coated NPs were produced using covalent conjugates of PLGA and LMWCs. PLGA-LMWC conjugates are graft polymers, in which LMWC makes up a backbone and multiple PLGA molecules are grafted as side chains. We envision that PLGA chains assemble to form a core, letting the relatively hydrophilic LMWC backbones form loops on the surface and face aqueous environment (Scheme 1). Although there was no visible sign of LMWC on the surface of PLGA-LMWC NPs in the SEM images, their positive surface charges at pH 6.2 reflect the formation of LMWC surface layer. Of the three NPs based on different MW LMWCs, PLGA-LMWC$_{2-4k}$ NP and PLGA-LMWC$_{4-6.5k}$ NP had particle sizes less than 200 nm, adequate for systemic administration.[27] PLGA-LMWC$_{11-22k}$ NP was more than twice larger than PLGA-LMWC$_{2-4k}$ NP or PLGA-LMWC$_{4-6.5k}$ NP. The difference may be explained by the length of chitosan loop between PLGA moieties. According to the estimation from the ninhydrin assay, all three PLGA-LMWCs had a comparable number of PLGA chains per LMWC molecule despite the different lengths of LMWCs. This means that PLGA-LMWC$_{11-22k}$ had particularly long intervals between PLGA molecules. The long chitosan chain may have formed a bulkier surface layer and increased the particle size. Alternatively, the relatively high MW of LMWC$_{11-22k}$ may have hindered the formation of denser NPs. Due to the large particle size, PLGA-LMWC$_{11-22k}$ NP was excluded from the subsequent cell studies.

PLGA-LMWC NPs displayed positive charges at pH 6.2, reflecting protonation of LMWC amines. On the other hand, they were slightly negatively charged at pH 7.4, due to the deprotonation of LMWC and the PLGA surface that was not completely covered by LMWCs. The pH responsiveness of surface charges of PLGA-LMWC NPs translated to differential NP-cell interactions at the two pHs. PLGA*-LMWC NPs had no interactions with SKOV-3 or NCI/ADR-RES cancer cells at pH 7.4 during the 3 hour incubation and were readily removed after washing. Conversely, PLGA*-LMWC NPs incubated at pH 6.2 remained with the cancer cells. PLGA* NPs had negative charges irrespective of pH, due to carboxyl termini exposed on the surface, and did not have significant interactions with cancer cells at either pH. The lack of cell-PLGA NP interactions was consistent with our previous report,[20] in which we demonstrated the inefficient cellular uptake of PLGA NP. The ability of PLGA-LMWC NP to cationize the surface at pH 6.2 and establish interactions

with cancer cells makes them attractive in drug delivery to acidic tumors. The lack of cellular interactions of PLGA-LMWC NPs at pH 7.4 appears to contrast with previous reports,[25, 26] in which PLGA NPs physically coated with chitosans are readily taken up by lung cancer cells. Since the medium pH was not specified in these studies, we are not certain if our results indeed contradict the previous findings. If the cellular uptake experiments were performed in pH 7.4, the difference might be attributable to relatively high MWs of the chitosans, which enhanced non-electrostatic interactions such as hydrogen bonding and hydrophobic interactions between the chitosan layer and cell membranes.

From microscopic images alone, it is not clear whether PLGA*-LMWC NP remained on the cell surface or were endocytosed by SKOV-3 cells. In either case, we expected that PLGA-LMWC NPs would be more efficient in delivering PTX and killing the cells at pH 6.2 as compared to those at pH 7.4 or PLGA NP. We did not observe the expected difference using the routine cell viability test protocol, where the cells were exposed to NPs for 72 hours. This may be due to the significant PTX release from the NPs in 12–24 hours. Both PTX/PLGA NP and PTX/PLGA-LMWC$_{2-4k}$ NP released >50% of total PTX in 24 hours in PBS containing 0.1% Tween 80, which we assumed resembled the extracellular environment. Therefore, cell killing was rather likely to be dictated by the already released PTX than that carried by the NPs. This is a significant weakness of these systems, especially when their promise in systemic drug delivery is predicated on the stability during circulation, and remains to be overcome in future studies. On the other hand, when the cell contact with the NPs was limited to 3 hours, when the drug release was relatively minimal (~10%), PTX/PLGA-LMWC$_{2-4k}$ NP at pH 6.2 showed significantly higher cytotoxicity than those at pH 7.4 and PTX/PLGA NP at both pHs in all tested concentrations. These results indicate that the electrostatic interactions between SKOV-3 cells and PTX/PLGA-LMWC$_{2-4k}$ NP established in the first 3 hours allowed the SKOV-3 cells to have a continued access to drug supplies during the subsequent incubation period. The ability of cationized PLGA-LMWC$_{2-4k}$ NP to deliver drugs through short-term exposure should allow them to serve as an effective drug delivery system to tumors, from which non-cell interactive NPs are constantly removed and returned to the circulation.

To evaluate the potential of LMWC as a stealth surface, we tested if PLGA-LMWC$_{2-4k}$ NP could avoid phagocytic uptake by macrophages and resist protein adsorption. Confocal microscopy shows that PLGA*-LMWC$_{2-4k}$ NP effectively avoided uptake by J774A.1 macrophages, whereas PLGA* NP was readily taken up by them. Of note, this result was obtained at pH 7.4, where both NPs were negatively charged; therefore, contribution of electrostatic interactions with cells to the cellular uptake was minimal for both NPs. We investigated if the LMWC surface was able to reduce protein adsorption on the particles, the first step of RES recognition and removal of circulating NPs.[28] Protein adsorption to the PLGA-LMWC mP was significantly lower than PLGA mP, although it was not as low as PLGA-PEG mP. Interestingly, PLGA-LMWC$_{4-6.5k}$ mP showed greater reduction in protein adsorption than PLGA-LMWC$_{2-4k}$ mP or PLGA-LMWC$_{11-22k}$ mP. The difference between PLGA-LMWC$_{4-6.5k}$ mP and PLGA-LMWC$_{2-4k}$ mP may be explained by the greater coverage of the mP surface by LMWC$_{4-6.5k}$, given the LMWC contents. However, PLGA-LMWC$_{11-22k}$ mP with even greater LMWC coverage showed higher protein adsorption than PLGA-LMWC$_{4-6.5k}$ mP. This may be due to the relatively hydrophobic nature of LMWC$_{11-22k}$ compared with the other LMWCs, suggested by the solubility profile (Fig. 1). Considering the LMWC content, hydrophilicity of the LMWC coating, particle size, and ability to interact with cells at acidic pH, PLGA-LMWC$_{4-6.5k}$ NP should be most appropriate for drug delivery to tumors.

In conclusion, this study shows that PLGA NPs coated with LMWCs have pH-sensitive cell interactions, which enable specific drug delivery to cells in a weakly acidic

microenvironment. The LMWCs provide hydrophilic layers on NP surface, reducing opsonization and phagocytic uptake. Due to these properties, LMWCs may be useful for both protecting NPs during circulation and enhancing their cellular uptake in a pH-sensitive manner. Chitosans have long been considered bioadhesive materials, which have great ability to interact with cells in general. However, this effect most likely depends on specific conditions, such as acidic environment and/or relatively high MW of chitosan. Here we showed that hydrophilic chitosans like LMWCs rather served as a non-fouling surface component than bioadhesive coating at a neutral pH. Recent studies using chitosans as a surface modifier in different contexts support the potential of chitosan as a stealth coating.[29–31] The utility of LMWC-coated NPs remains to be demonstrated through *in vivo* pharmacokinetics and biodistribution studies, currently ongoing in our laboratory.

Supplementary Material

Refer to Web version on PubMed Central for supplementary material.

Acknowledgments

REFERENCES

1. Kirpotin DB, Drummond DC, Shao Y, Shalaby MR, Hong KL, Nielsen UB, Marks JD, Benz CC, Park JW. Antibody targeting of long-circulating lipidic nanoparticles does not increase tumor localization but does increase internalization in animal models. Cancer Res. 2006; 66:6732–6740. [PubMed: 16818648]

2. Mamot C, Drummond DC, Noble CO, Kallab V, Guo ZX, Hong KL, Kirpotin DB, Park JW. Epidermal growth factor receptor-targeted immunoliposomes significantly enhance the efficacy of multiple anticancer drugs in vivo. Cancer Res. 2005; 65:11631–11638. [PubMed: 16357174]

3. Bartlett DW, Su H, Hildebrandt IJ, Weber WA, Davis ME. Impact of tumor-specific targeting on the biodistribution and efficacy of siRNA nanoparticles measured by multimodality in vivo imaging. Proc. Natl. Acad. Sci. U.S.A. 2007; 104:15549–15554. [PubMed: 17875985]

4. Moreno D, Zalba S, Navarro I, Tros de Ilarduya C, Garrido MJ. Pharmacodynamics of cisplatin-loaded PLGA nanoparticles administered to tumor-bearing mice. Eur. J. Pharm. Biopharm. 2010; 74:265–274. [PubMed: 19883755]

5. Carrstensen H, Müller RH, Müller BW. Particle size, surface hydrophobicity and interaction with serum of parenteral fat emulsions and model drug carriers as parameters related to RES uptake. Clin Nutr. 1992; 11:289–297. [PubMed: 16840011]

6. Otsuka H, Nagasaki Y, Kataoka K. PEGylated nanoparticles for biological and pharmaceutical applications. Adv. Drug Deliv Rev. 2003; 55:403–419. [PubMed: 12628324]

7. Huang C, Neoh KG, Wang LA, Kang ET, Shuter B. Magnetic nanoparticles for magnetic resonance imaging: modulation of macrophage uptake by controlled PEGylation of the surface coating. J. Mater. Chem. 2010; 20:8512–8520.

8. Mishra S, Webster P, Davis ME. PEGylation significantly affects cellular uptake and intracellular trafficking of non-viral gene delivery particles. Eur. J. Cell Biol. 2004; 83:97–111. [PubMed: 15202568]

9. Romberg B, Hennink W, Storm G. Sheddable Coatings for Long-Circulating Nanoparticles. Pharmaceut.l res. 2008; 25:55–71.

10. Hong RL, Huang CJ, Tseng YL, Pang VF, Chen ST, Liu JJ, Chang FH. Direct comparison of liposomal doxorubicin with or without polyethylene glycol coating in C-26 tumor-bearing mice: Is surface coating with polyethylene glycol beneficial? Clin. Cancer Res. 1999; 5:3645–3652. [PubMed: 10589782]

11. Hatakeyama H, Akita H, Harashima H. A multifunctional envelope type nano device (MEND) for gene delivery to tumours based on the EPR effect: A strategy for overcoming the PEG dilemma. Adv. Drug Deliv Rev. 2011; 63:152–160. [PubMed: 20840859]

12. Wolf BB, Otto AMA, Brischwein MM, Kraus MM, Henning TT. Relevance of tumor microenvironment for progression, therapy and drug development. Anti-Cancer Drugs. 2004; 15:7–14. [PubMed: 15090737]

13. Gerweck LE, Seetharaman K. Cellular pH Gradient in Tumor versus Normal Tissue: Potential Exploitation for the Treatment of Cancer. Cancer Res. 1996; 56:1194–1198. [PubMed: 8640796]

14. Tannock IF, Rotin D. Acid pH in tumors and its potential for therapeutic exploitation. Cancer Res. 1989; 49:4373–4384. [PubMed: 2545340]

15. Sawant RM, Hurley JP, Salmaso S, Kale A, Tolcheva E, Levchenko TS, Torchilin VP. "SMART" drug delivery systems: Double-targeted pH-responsive pharmaceutical nanocarriers. Bioconjugate Chem. 2006; 17:943–949.

16. Cheng R, Feng F, Meng F, Deng C, Feijen J, Zhong Z. Glutathione-responsive nano-vehicles as a promising platform for targeted intracellular drug and gene delivery. J. Controlled Release. 2011; 152:2–12.

17. Nie Y, Günther M, Gu Z, Wagner E. Pyridylhydrazone-based PEGylation for pH-reversible lipopolyplex shielding. Biomaterials. 2010; 32:858–869. [PubMed: 21030074]

18. Sethuraman VA, Bae YH. TAT peptide-based micelle system for potential active targeting of anti-cancer agents to acidic solid tumors. J. Controlled Release. 2007; 118:216–224.

19. Leane MM, Nankervis R, Smith A, Illum L. Use of the ninhydrin assay to measure the release of chitosan from oral solid dosage forms. Int. J. Pharm. 2004; 271:241–249. [PubMed: 15129991]

20. Xu P, Gullotti E, Tong L, Highley CB, Errabelli DR, Hasan T, Cheng J-X, Kohane DS, Yeo Y. Intracellular Drug Delivery by Poly(lactic-co-glycolic acid) Nanoparticles, Revisited. Mol. Pharmaceutics. 2009; 6:190–201.

21. Tian F, Liu Y, Hu KA, Zhao BY. Study of the depolymerization behavior of chitosan by hydrogen peroxide. Carbohyd. Polym. 2004; 57:31–37.

22. Muzzarelli, RAA.; Peter, MG.; Society, EC. Chitin handbook. Atec; 1997. p. 457-566.

23. He P, Davis SS, Illum L. In vitro evaluation of the mucoadhesive properties of chitosan microspheres. Int. J. Pharm. 1998; 166:75–88.

24. Lehr C-M, Bouwstra JA, Schacht EH, Junginger HE. In vitro evaluation of mucoadhesive properties of chitosan and some other natural polymers. Int. J. Pharm. 1992; 78:43–48.

25. Tahara K, Sakai T, Yamamoto H, Takeuchi H, Hirashima N, Kawashima Y. Improved cellular uptake of chitosan-modified PLGA nanospheres by A549 cells. Int. J. Pharm. 2009; 382:198–204. [PubMed: 19646519]

26. Kim B-S, Kim C-S, Lee K-M. The intracellular uptake ability of chitosan-coated Poly (D,L-lactideco-glycolide) nanoparticles. Arch. Pharmacal Res. 2008; 31:1050–1054.

27. Zhang L, Gu FX, Chan JM, Wang AZ, Langer RS, Farokhzad OC. Nanoparticles in medicine: Therapeutic applications and developments. Clin. Pharmacol. Ther. 2008; 83:761–769. [PubMed: 17957183]

28. Owens DE, Peppas NA. Opsonization, biodistribution, and pharmacokinetics of polymeric nanoparticles. Int. J. Pharm. 2006; 307:93–102. [PubMed: 16303268]

29. Zhou J, Romero G, Rojas E, Ma L, Moya S, Gao C. Layer by layer chitosan/alginate coatings on poly(lactide-co-glycolide) nanoparticles for antifouling protection and Folic acid binding to achieve selective cell targeting. J. Colloid Interface Sci. 2010; 345:241–247.

30. Sarmento B, Mazzaglia D, Bonferoni MC, Neto AP, do Céu Monteiro M, Seabra V. Effect of chitosan coating in overcoming the phagocytosis of insulin loaded solid lipid nanoparticles by mononuclear phagocyte system. Carbohyd. Polym. 2011; 84:919–925.

31. Chung Y-I, Kim JC, Kim YH, Tae G, Lee S-Y, Kim K, Kwon IC. The effect of surface functionalization of PLGA nanoparticles by heparin- or chitosan-conjugated Pluronic on tumor targeting. J. Controlled Release. 2010; 143:374–382.
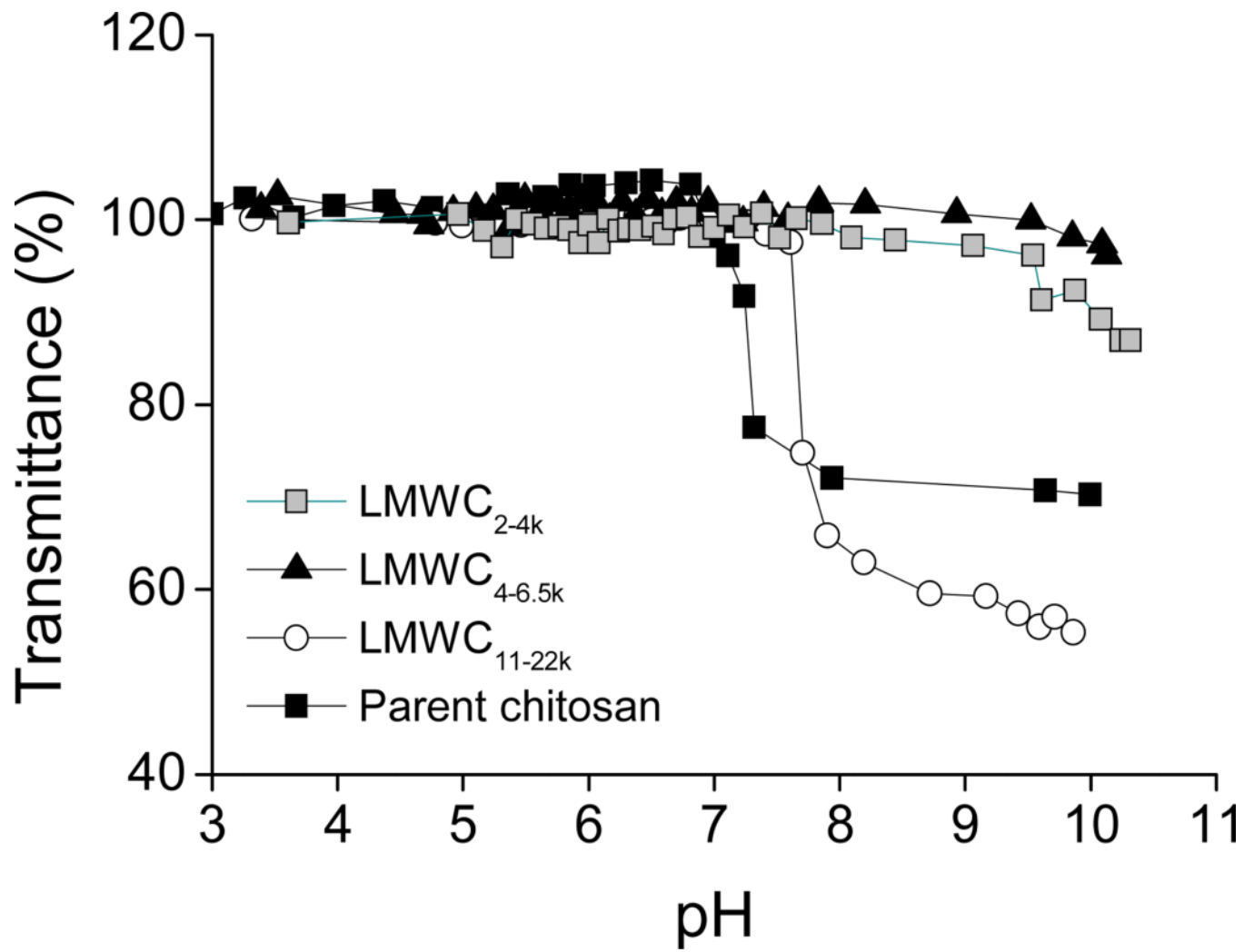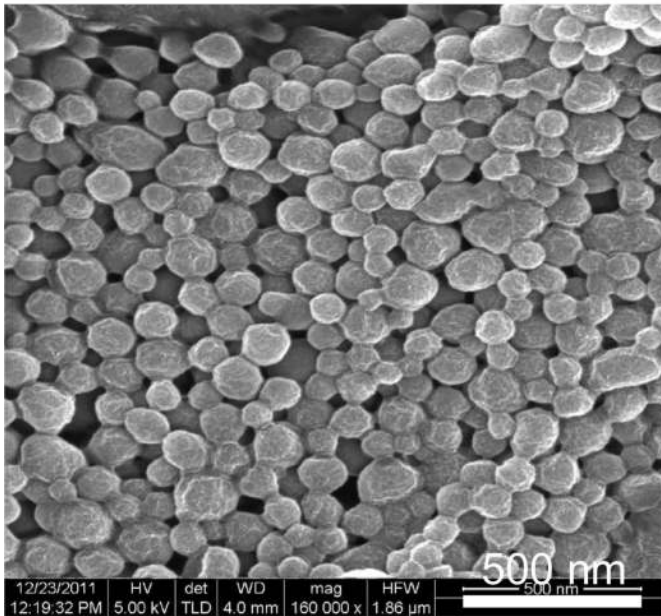
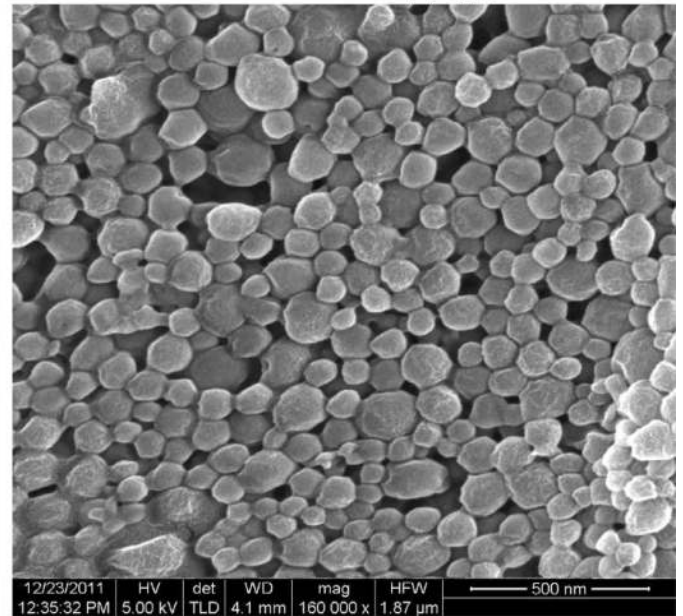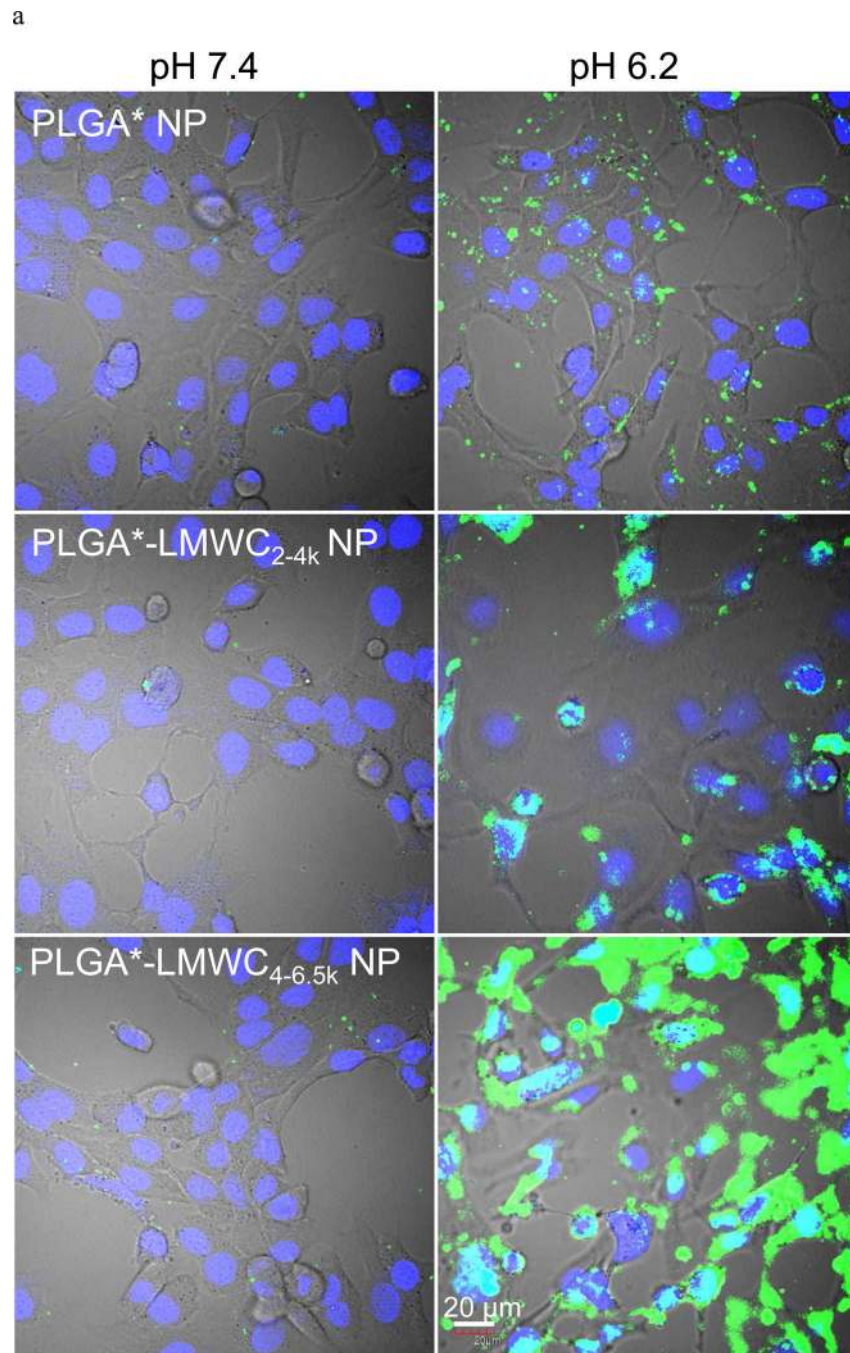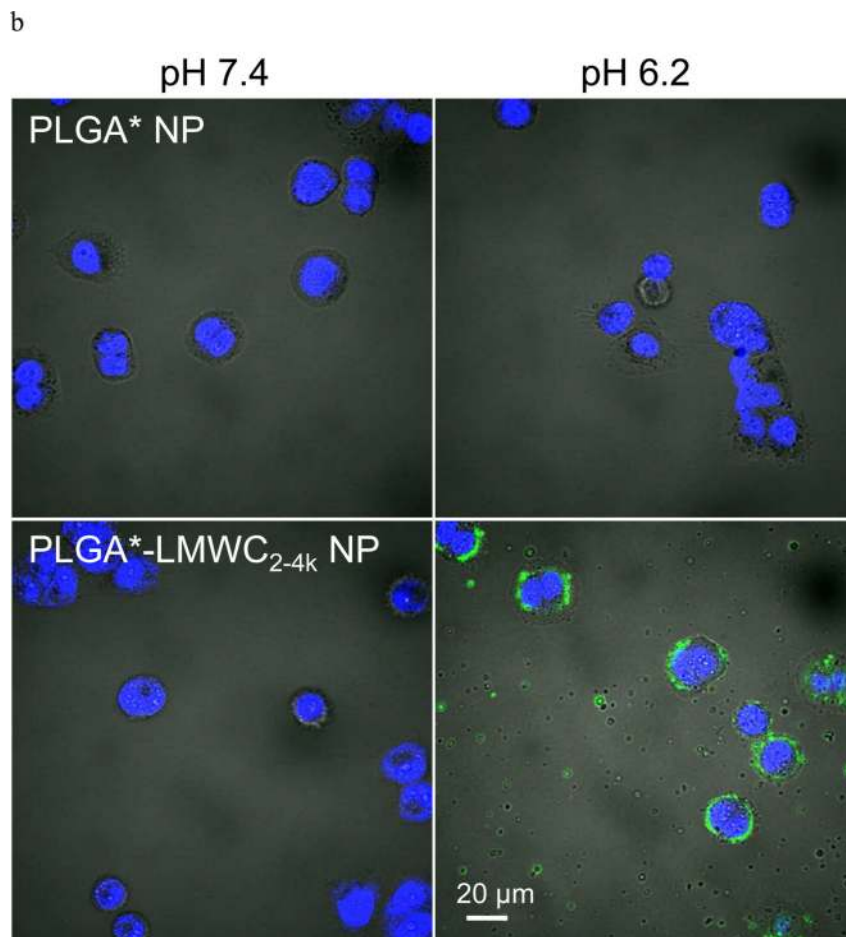**Fig. 1.**
pH-dependent transmittance change of chitosans
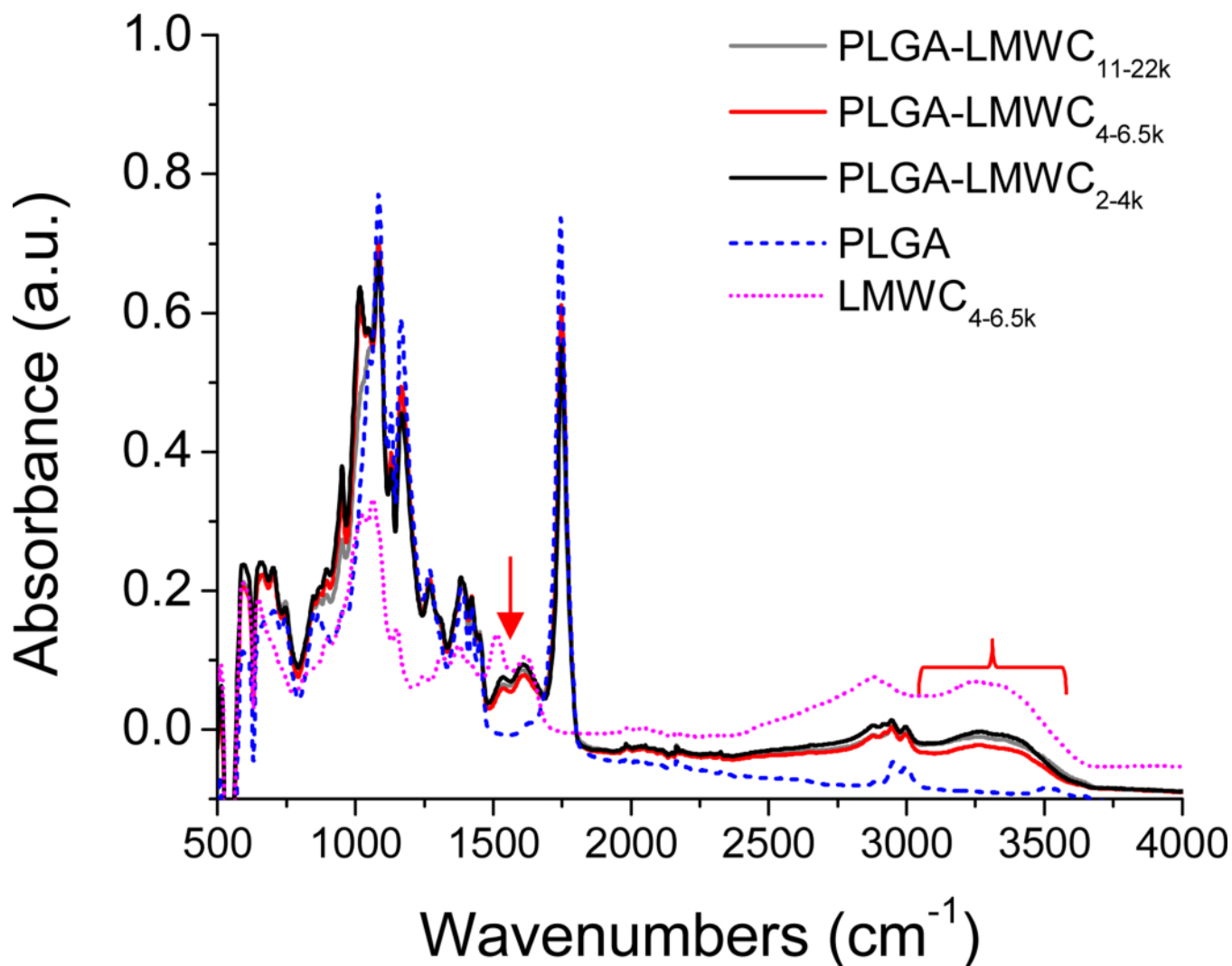
Fig. 2.
FTIR spectroscopy of PLGA-LMWCs, PLGA and LMWC$_{4–6.5k}$. The presence of amide and amine bands (arrow, 1500–1690 cm^{-1}) and a broad N-H signal (brace, 3000–3700 cm^{-1}) confirms the conjugation of LMWC to PLGA.

PLGA NPs

PLGA-LMWC$_{2-4k}$ NPs

Fig. 3.
Scanning electron microscope images of PLGA NPs and PLGA-LMWC$_{2–4k}$ NPs.

a

Fig. 4.
pH dependence of cellular association of PLGA* NPs and PLGA*-LMWC NPs. Confocal images of (a) SKOV-3 ovarian cancer cells or (b) NCI/ADR-RES multidrug resistant ovarian cancer cells were taken after 3-hour incubation with the NPs (overlaid images of NP (green), nuclei (blue), and transmission images).

# PLGA* NP

PLGA*-LMWC$_{2\text{-}4k}$ NP
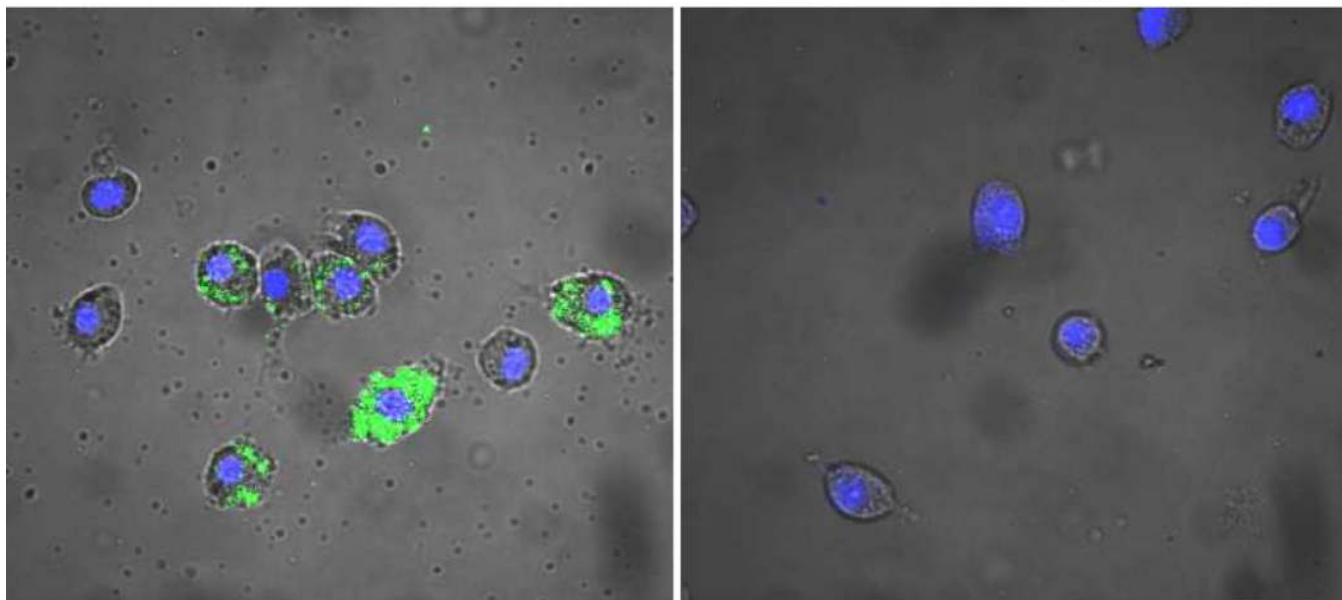
Fig. 5.
J774A.1 macrophages incubated with PLGA* NPs or PLGA*-LMWC$_{2-4k}$ NPs for 3 hours
at pH 7.4. Overlaid images of NP (green), nuclei (blue), and transmission images.

a

b
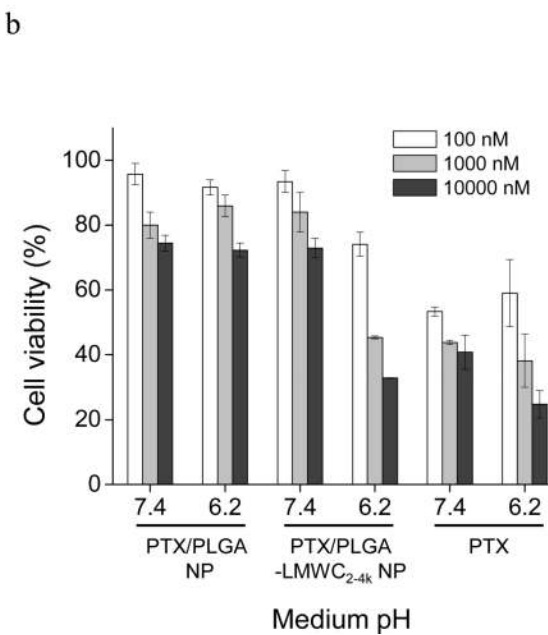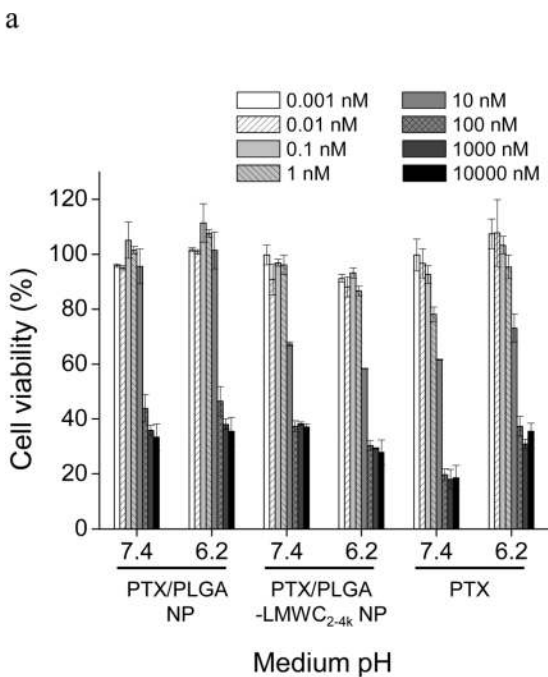
Fig. 6.
Viability of SKOV-3 cells exposed to PTX or PTX/NPs at different pHs for (a) 72 hours or (b) 3 hours. Data are expressed as averages with standard deviations of 4 identically and independently prepared samples.
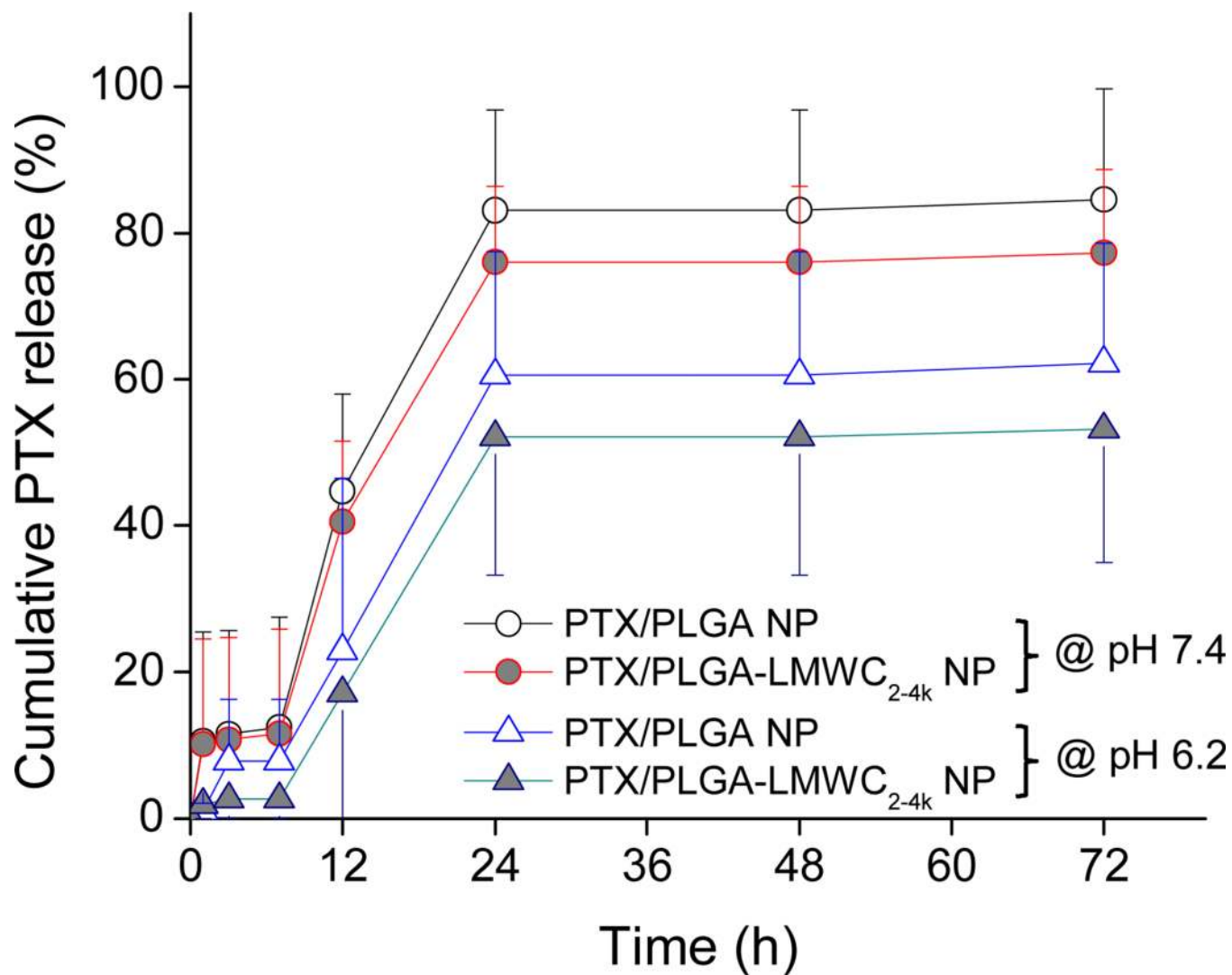
Fig. 7.
In vitro release of PTX from NPs. There was no difference across the samples at each time point (p>0.05 with ANOVA). Data are expressed as averages with standard deviations of 3 identically and independently prepared samples. For the clarity of presentation, error bars are shown in one direction.
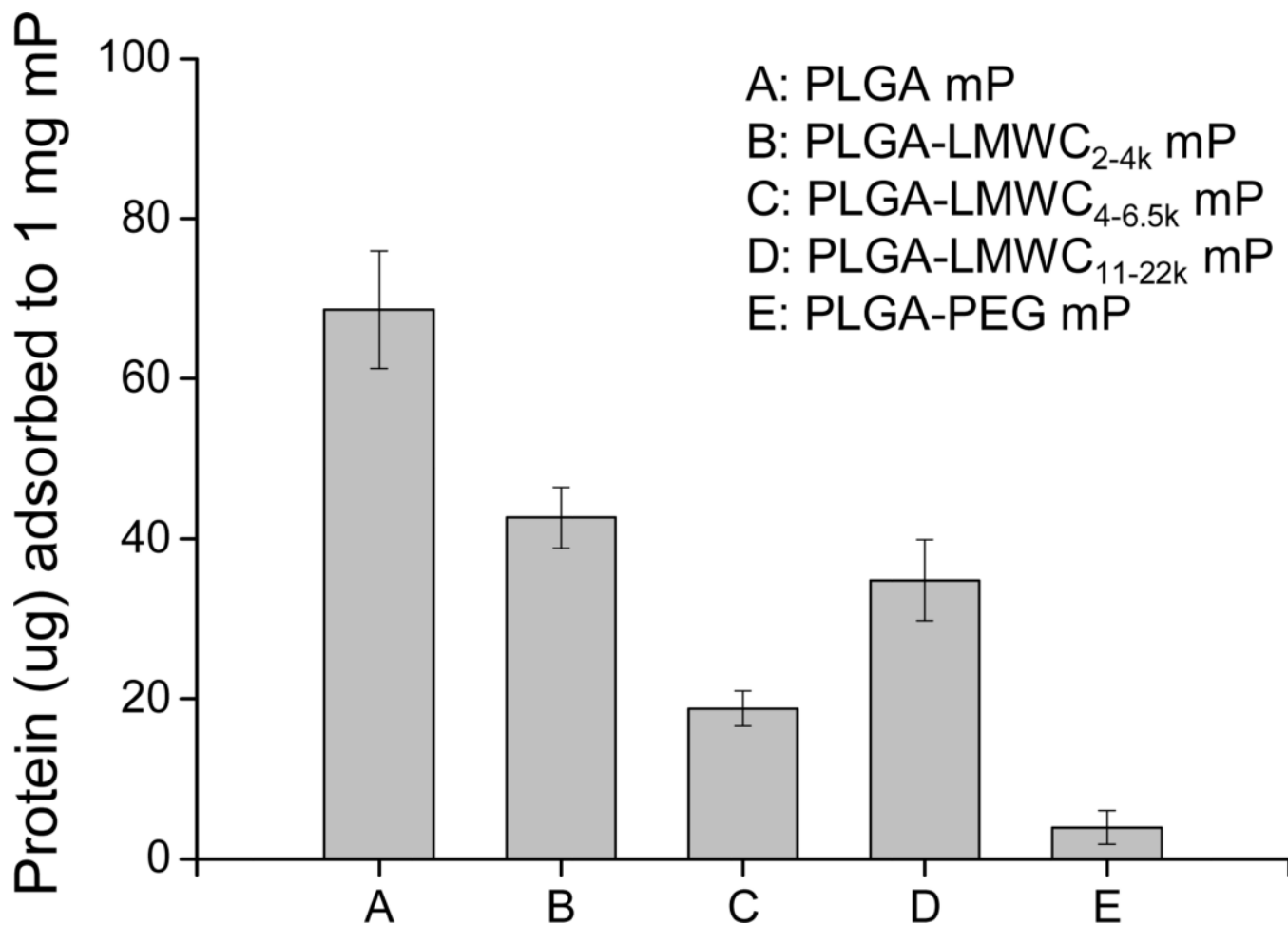
Fig. 8.
Protein adsorbed to 1 mg PLGA mPs or PLGA-LMWC mPs. All samples are significantly different from each other with p values less than 0.001, except for PLGA-LMWC$_{2-4k}$ mPs vs. PLGA-LMWC$_{11-22k}$ mPs (p<0.05). Data are expressed as averages with standard deviations of 6 identically and independently prepared samples.
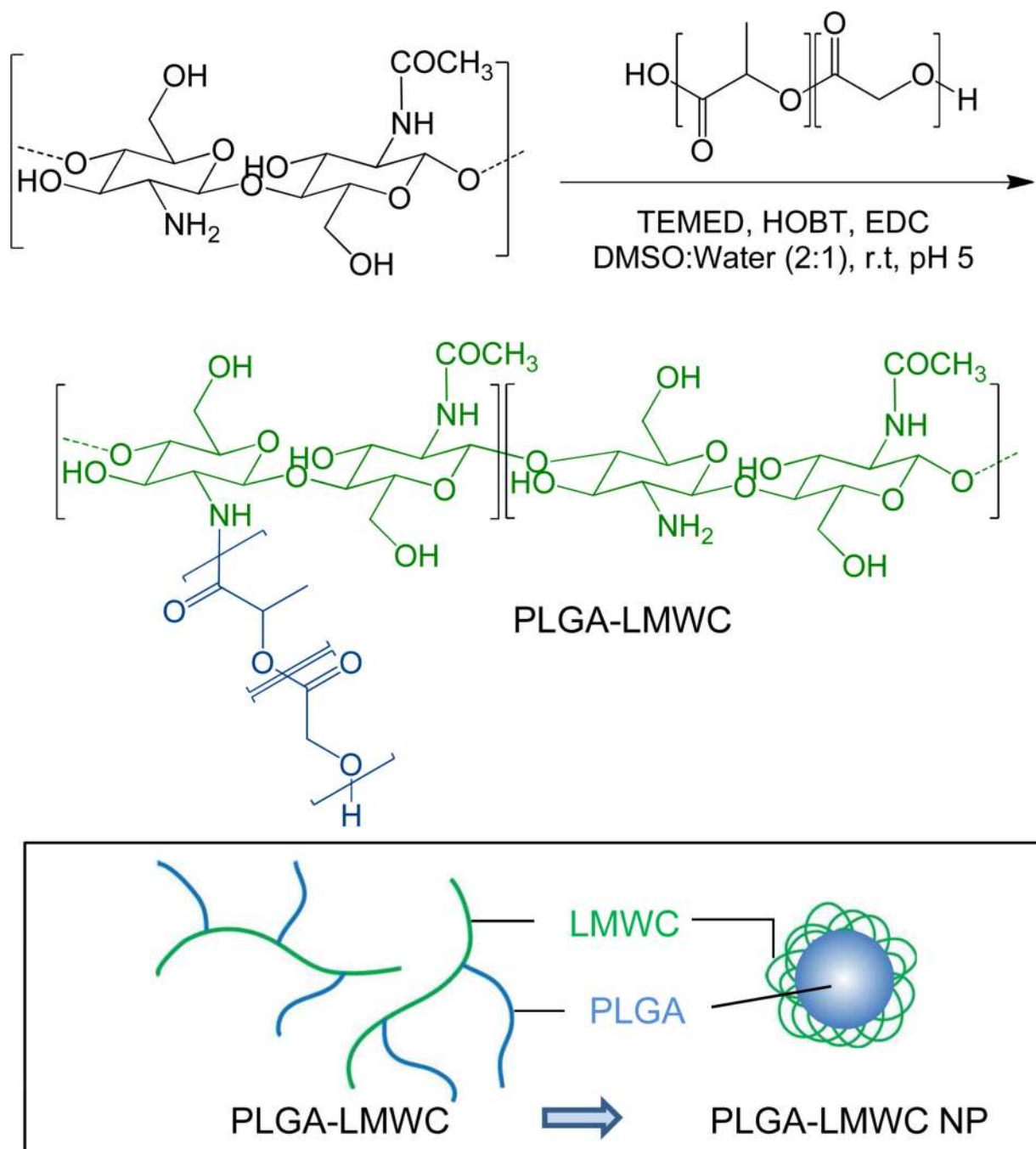
Scheme 1.
Synthesis of PLGA-LMWC and schematic diagram of PLGA-LMWC NP

Table 1

Particle size and surface charge of NPs[a]

	pH 7.4			pH 6.2		
	Size (nm)	PD[b]	Zeta (mV)	Size (nm)	PD[b]	Zeta (mV)
PLGA NP	177.5 ± 40.2	0.15 ± 0.1	−11.1 ± 3.1	191.6 ± 43.2	0.09 ± 0.01	−14.6 ± 4.3
PLGA/LMWC$_{15k}$ NP	175 ± 12.0	0.25 ± 0.07	−12.0 ± 2.0	184.1 ± 11.5	0.29 ± 0.02	−10.1 ± 1.8
PLGA-LMWC$_{2-4k}$ NP	176.0 ± 45.2	0.23 ± 0.09	−6.0 ± 2.3	183.3 ± 47.4	0.10 ± 0.01	+3.3 ± 1.4
PLGA-LMWC$_{4-6.5k}$ NP	191.6 ± 34.1	0.18 ± 0.01	−4.4 ± 1.2	198.8 ± 28.9	0.13 ± 0.02	+5.5 ± 1.9
PLGA-LMWC$_{11-22k}$ NP	480.0 ± 21.0	0.17 ± 0.04	−9.3 ± 4.0	404.1 ± 31.3	0.12 ± 0.06	+14.9 ± 0.9

[a]Data are expressed as averages and standard deviations of 6 independent batches, except for PLGA/LMWC NP (n=3).

[b]PD: Polydispersity, an estimate of the width of the particle size distribution, obtained from the cumulants analysis as described in the International Standard on DLS ISO13321 Part 8 (Malvern DLS technical note MRK656-01). PD <0.08 is considered monodisperse.